Electronic Supplementary Information

Electrolyte Engineering for Effective Seawater Splitting Based on Manganese Iron Chromium Layered Triple Hydroxides as Novel Bifunctional Electrocatalysts

Santanu Pal,[a,b] Koji Shimizu,[c] Sakila Khatun,[a,b] Soumen Singha,[d] Satoshi Watanabe,[c]* Poulomi Roy[a,b]*

[a]Materials Processing & Microsystems Laboratory, CSIR – Central Mechanical Engineering Research Institute (CMERI), Mahatma Gandhi Avenue, Durgapur 713209, West Bengal, India

[b]Academy of Scientific and Innovative Research (AcSIR), CSIR- Human Resource Development Centre (CSIR-HRDC), Ghaziabad, Uttar Pradesh- 201 002, India.
E-mail: poulomiroy@yahoo.com

[c]Department of Materials Engineering, The University of Tokyo, 7-3-1 Hongo, Bunkyo-ku, Tokyo 113-8656, Japan
E-mail: watanabe@cello.t.u-tokyo.ac.jp

[d]Department of Physics, Jadavpur University, Kolkata-700032, India

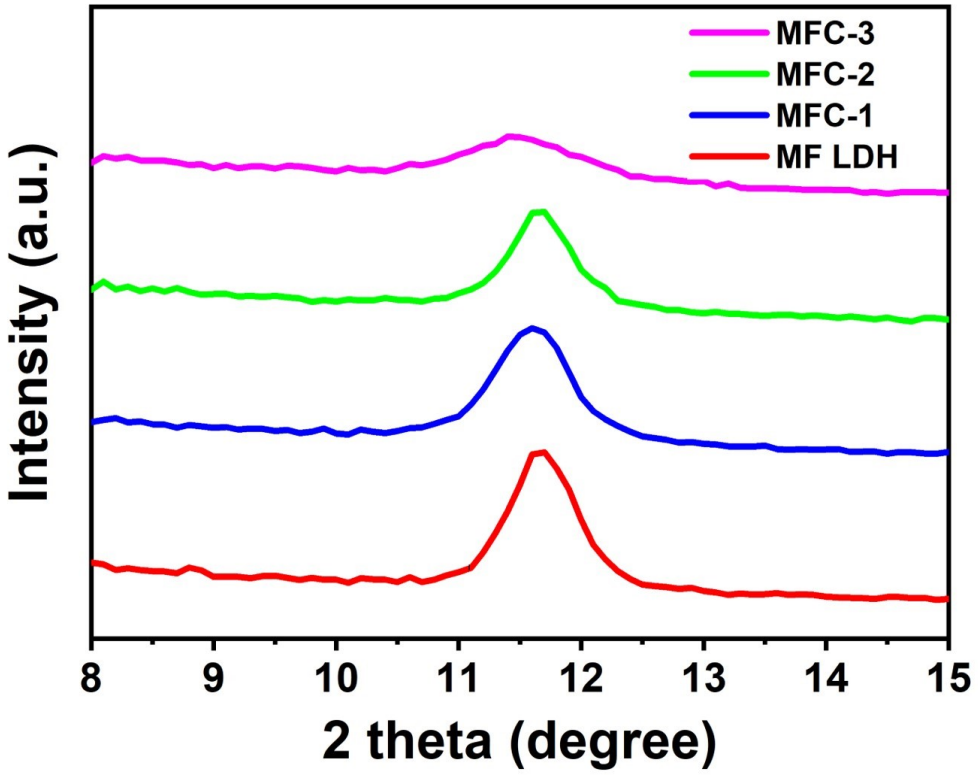

Figure S1. Enlarged view of XRD peak at 11.6°.

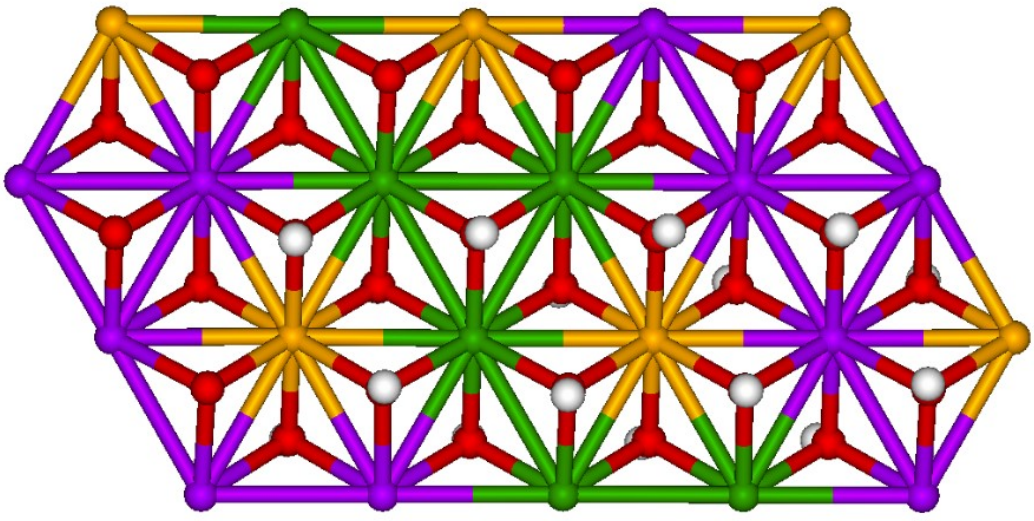

Figure S2. layered Structure of MnFeCr triple hydroxide (Fe: Orange, Mn: Pink, Cr: Green, O: Red and H: White).

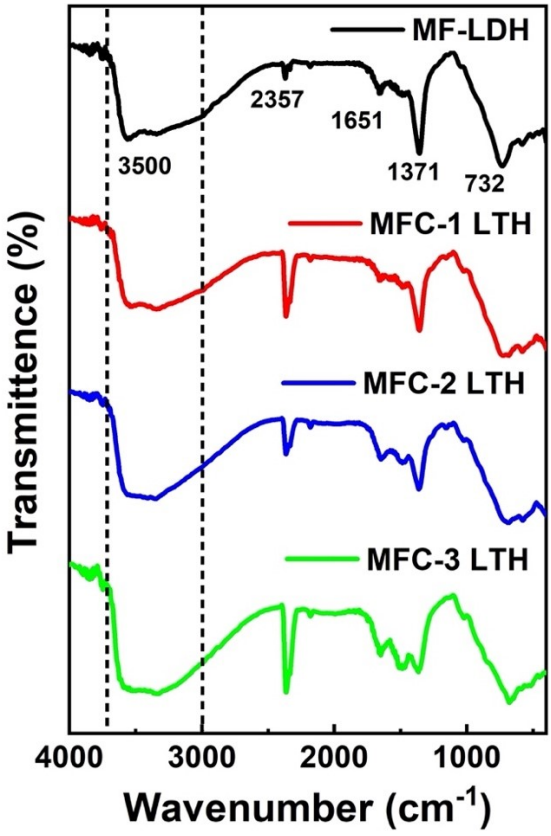

Figure S3. FTIR spectra for MF-LDH and MFC LTH samples.

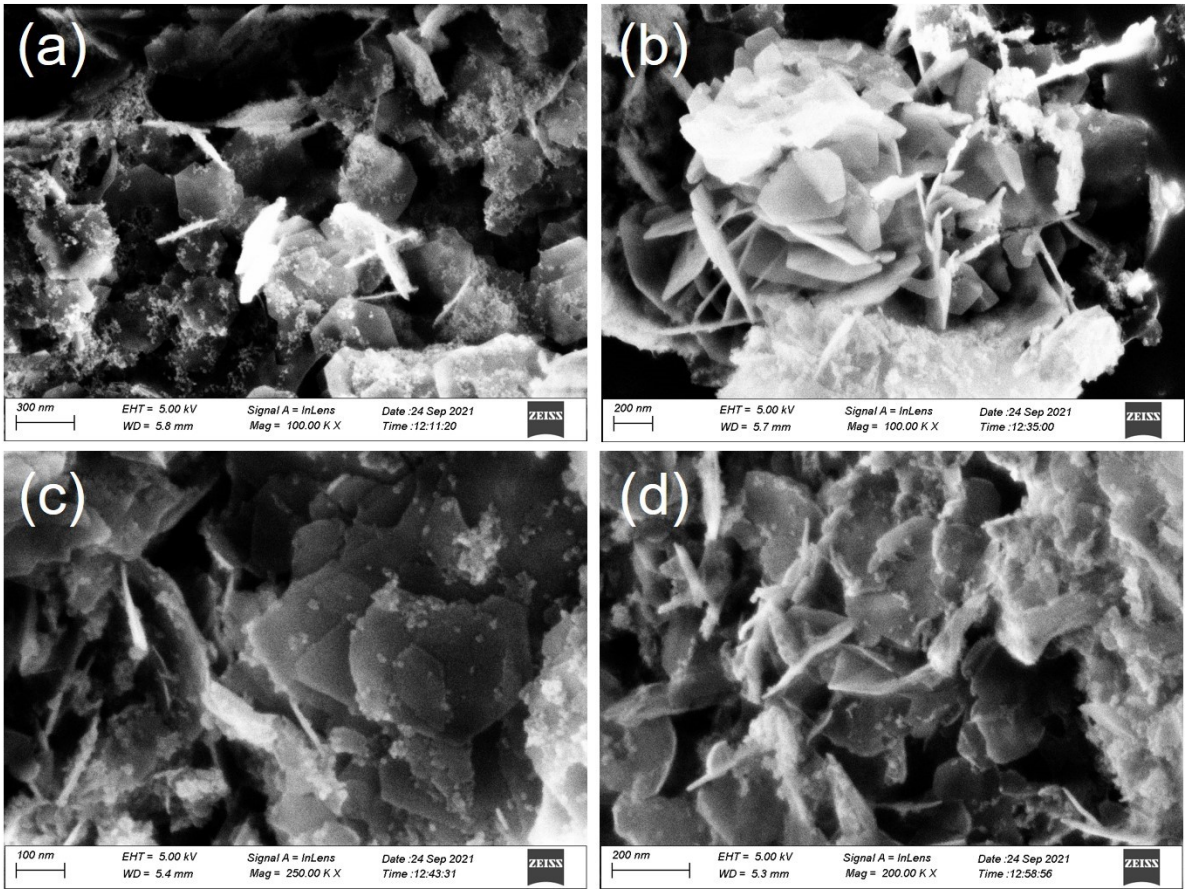

Figure S4. FESEM images of MF (a), MFC-1 (b), MFC-2 (c) and MFC-3 (d) samples.

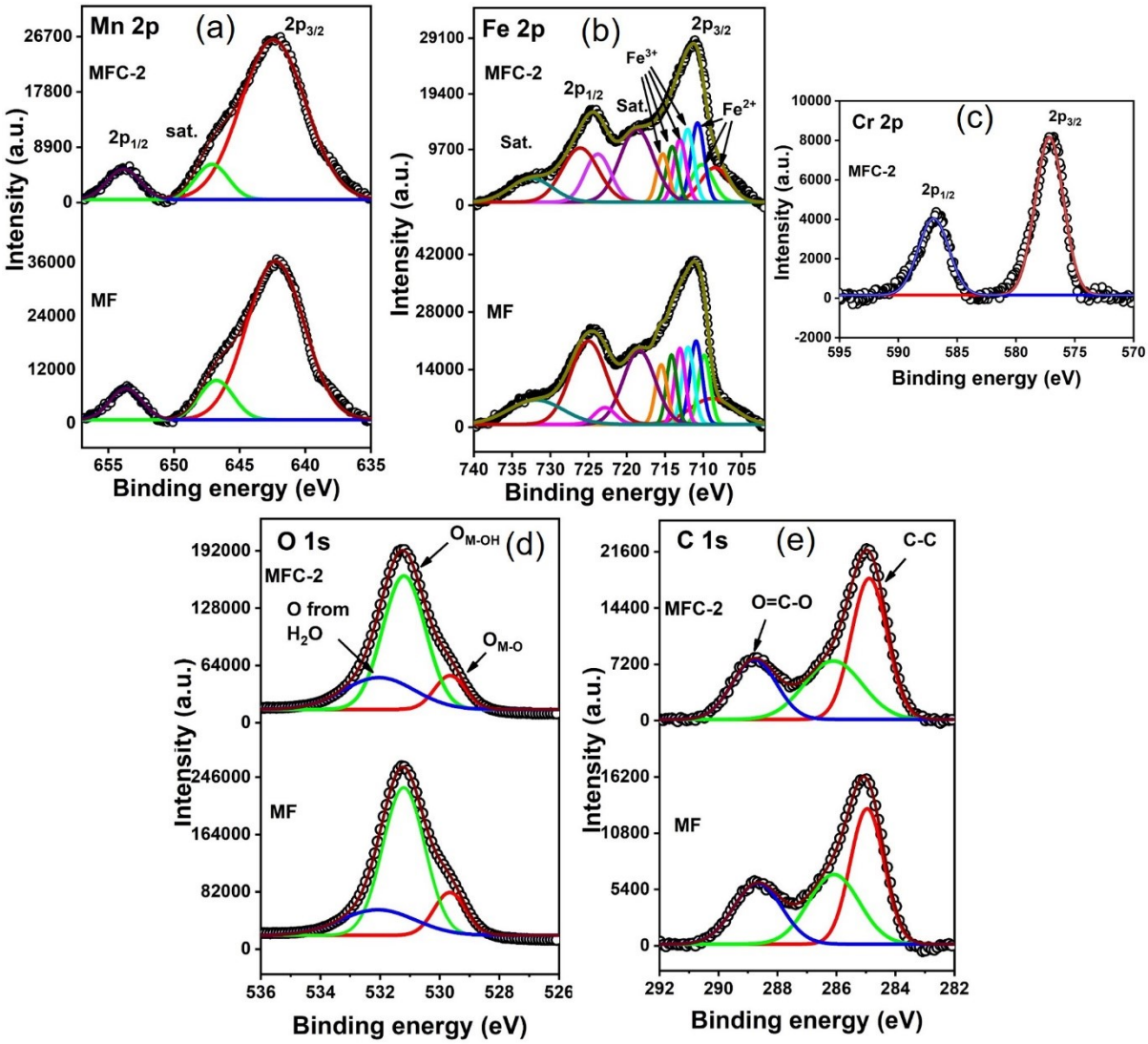

Figure S5. High resolution XPS analysis of (a) Mn 2*p*, (b) Fe 2*p*, (c) Cr 2*p*, (d) O 1*s* and (e) C 1*s* for MF and MFC-2 samples.

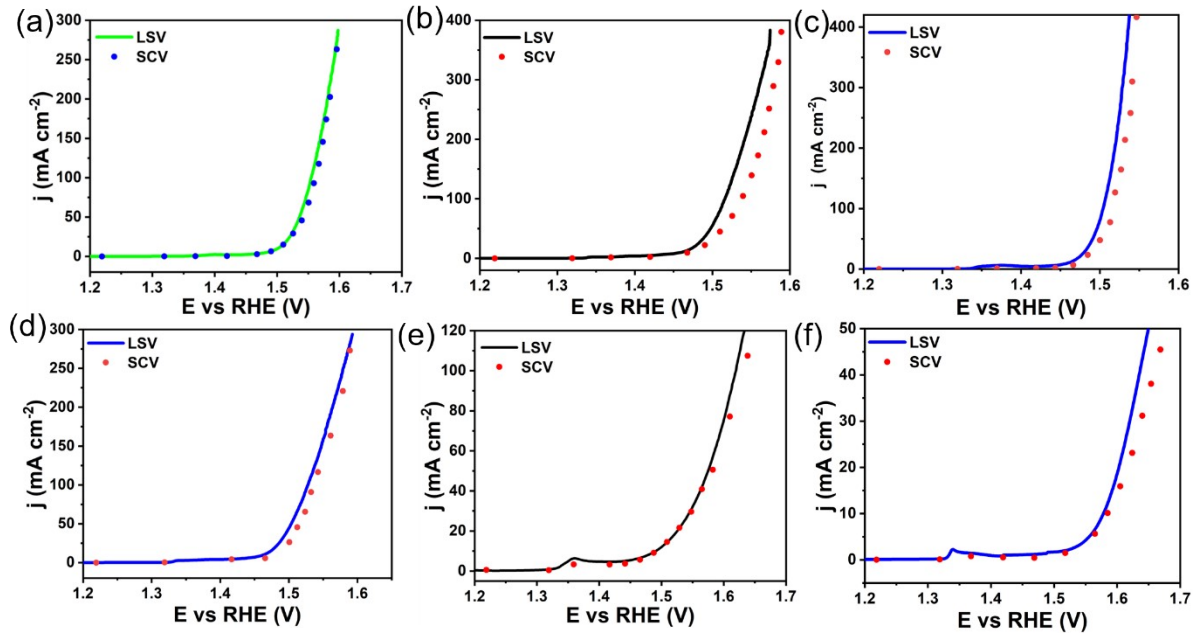

Figure S6. Comaprison of LSV and SCV plot for (a) MF LDH, (b) MFC-1, (c) MFC-2, (d) MFC-3, (e) RuO_2 and (f) bare NF electrocatalysts showing their performance towards OER activity.

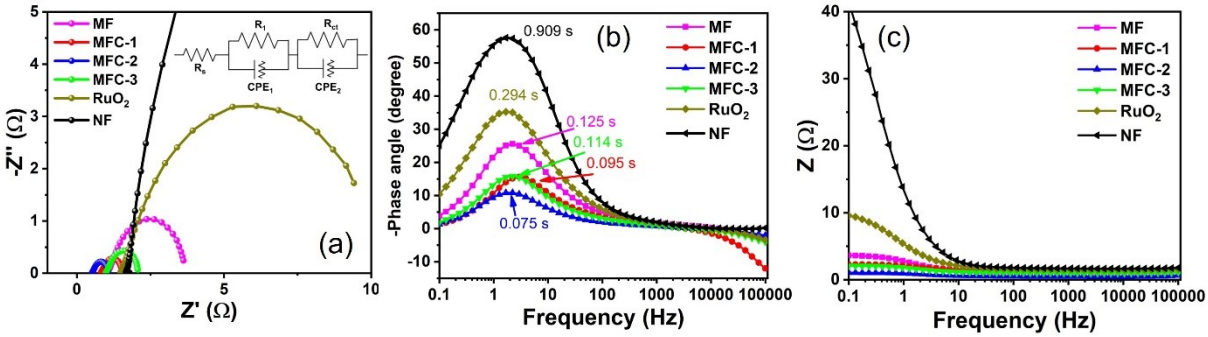

Figure S7. (a) PEIS taken at 1.518 V vs RHE from 100 kHz – 0.1 Hz for OER of as prepared LDH, LTHs, RuO_2 and NF in 1M KOH electrolyte medium. (b) Bode Phase angle plot and (c) Bode plot of electrocatalysts taken in 1M KOH electrolyte of corresponding electrocatalysts.

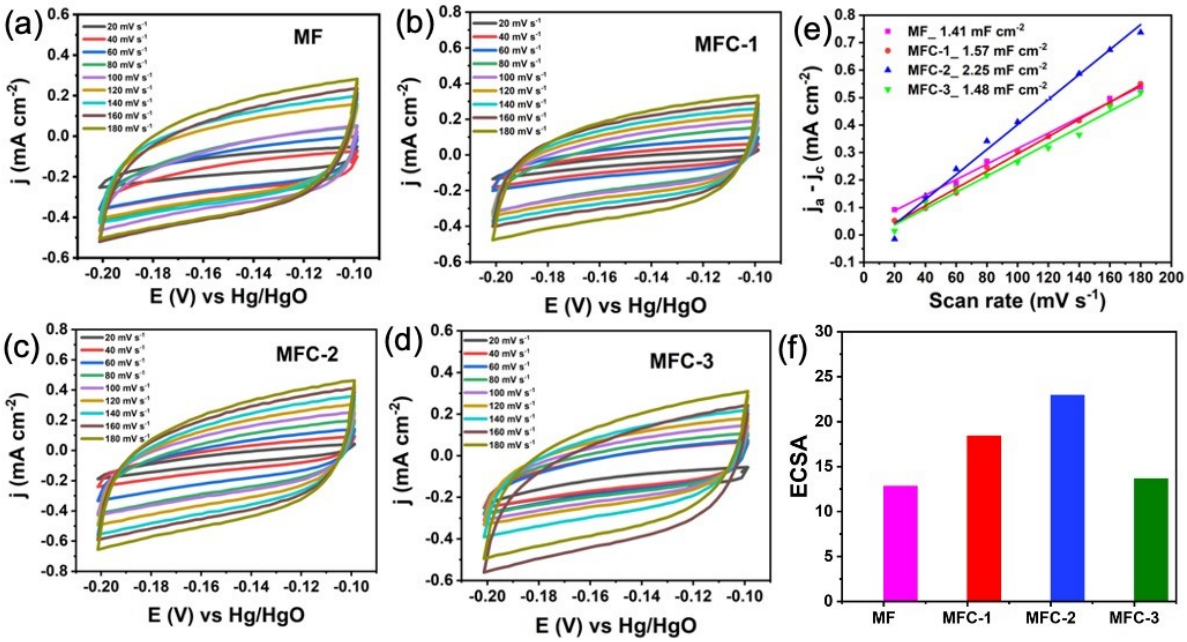

Figure S8. (a-d) Cyclic voltammogram plots in non-Faradic region for (a) MF, (b) MFC-1, (c) MFC-2 and (d) MFC-3 in 1M KOH electrolyte and (e) calculated C_{dl} values. (f) ECSA values of corresponding LDH and LTHs.

Determination of specific capacitance:

Capacitance = Charge/potential

Considering MF-LDH as an example, the area calculated from CV at scan rate of 20 mV s^{-1} = 1.37 × 10^{-8} AV

Associated charge = integrated area / (2 × scan rate)

= (1.37 × 10^{-8} AV) / (2 × 0.02 V s^{-1})

= 3.42 × 10^{-7} A s

= 3.42 × 10^{-7} C

Specific capacitance = charge / (area of electrode × potential window)

= 110 μF cm^{-2}

The C_s values for MFC-1, MFC-2 and MFC-3 LTHs were calculated in similar way.

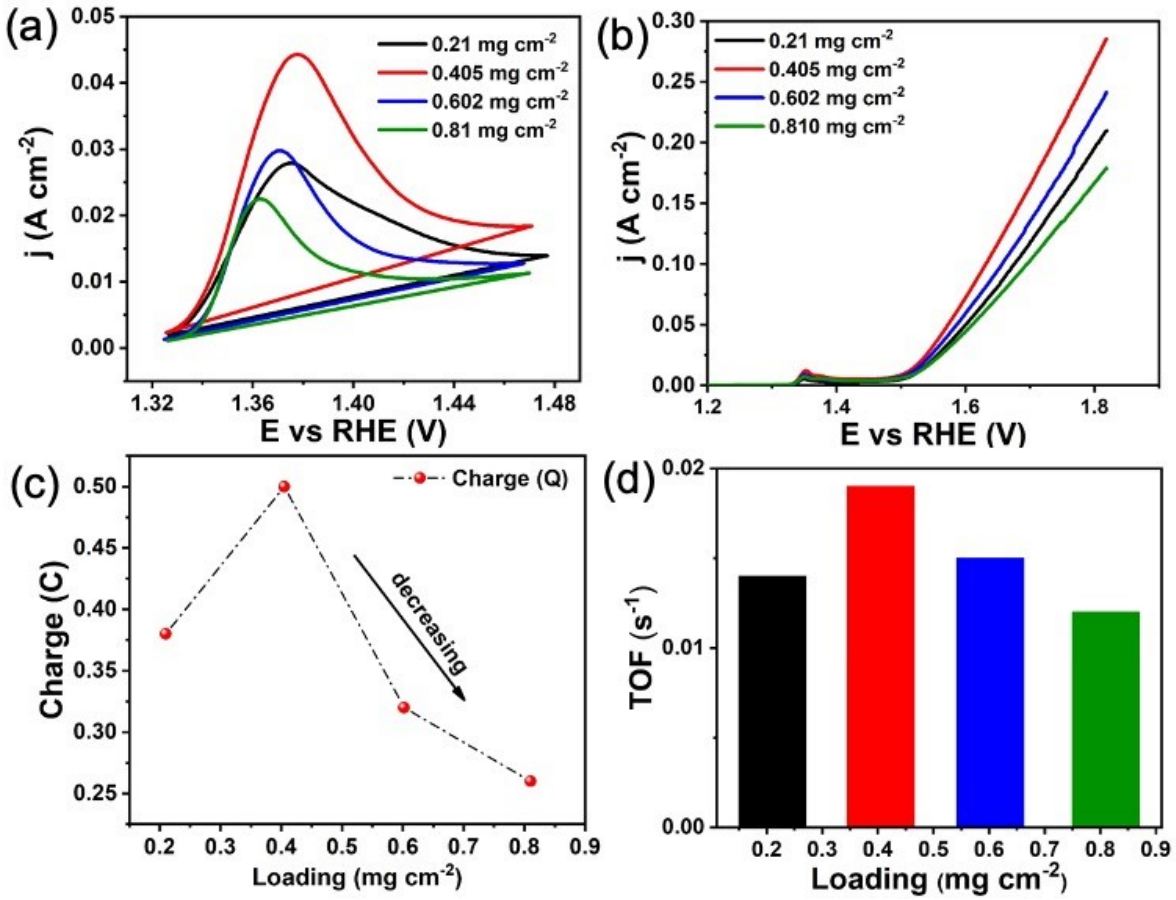

Figure S9. Mass loading optimization of MF: (a) Oxidation peak area, (b) iR drop uncompensated LSV, (c) charge associated to oxidation and (d) calculated TOF of MF-LDH at different mass loading at η_{300}.

TOF Calculations:

To calculate TOF, four different mass loading, 0.21, 0.405, 0.62 and 0.81 mg cm^{-2} for electrocatalysts were considered to identify the optimum mass loading to attain near-perfect monolayer. As an example, we show here the mass loading optimization for MF-LDH and TOF calculation thereof.

First we evaluated the area under the oxidation peak indicating the participating active sites for TOF calculation and the number of electron involved during oxidation reaction of active species. In all cases, CVs were analysed at 10 mV s^{-1} scan rate.

For MF-LDH with 0.21 mg cm^{-2} mass loading:

Area under oxidation peak = 3.8×10^{-3} AV.

Hence, associated charge with oxidation peak of real active sites (Qs) = 3.8×10^{-3} AV / 0.01 V s^{-1} = 0.38 As = 0.38 C

The number of transferred electrons are the equivalent to the no. of total active sites.

Hence, no. of moles of active sites that involved in OER (*m*) = *Qs* / *F*

$$= 0.38 \text{ C} / 96485 \text{ C mol}^{-1}$$

TOF at 1.53 V (300 mV overpotential) vs. RHE for MF LDH with mass loading of 0.21 mg cm^{-2} is

$(TOF)_{300\ mV} = 0.021 \text{ A} / [4 \times 96485 \text{ C mol}^{-1} \times (0.38 \text{ C} / 96485 \text{ C mol}^{-1})]$

$= 0.0138 \text{ s}^{-1}$

The TOF for MF LDH was calculated with mass loading of 0.405 mg cm^{-2}, 0.602 mg cm^{-2} and 0.81 mg cm^{-2} respectively and was found to be 0.019 s^{-1}, 0.0158 s^{-1} and 0.0127 s^{-1}.

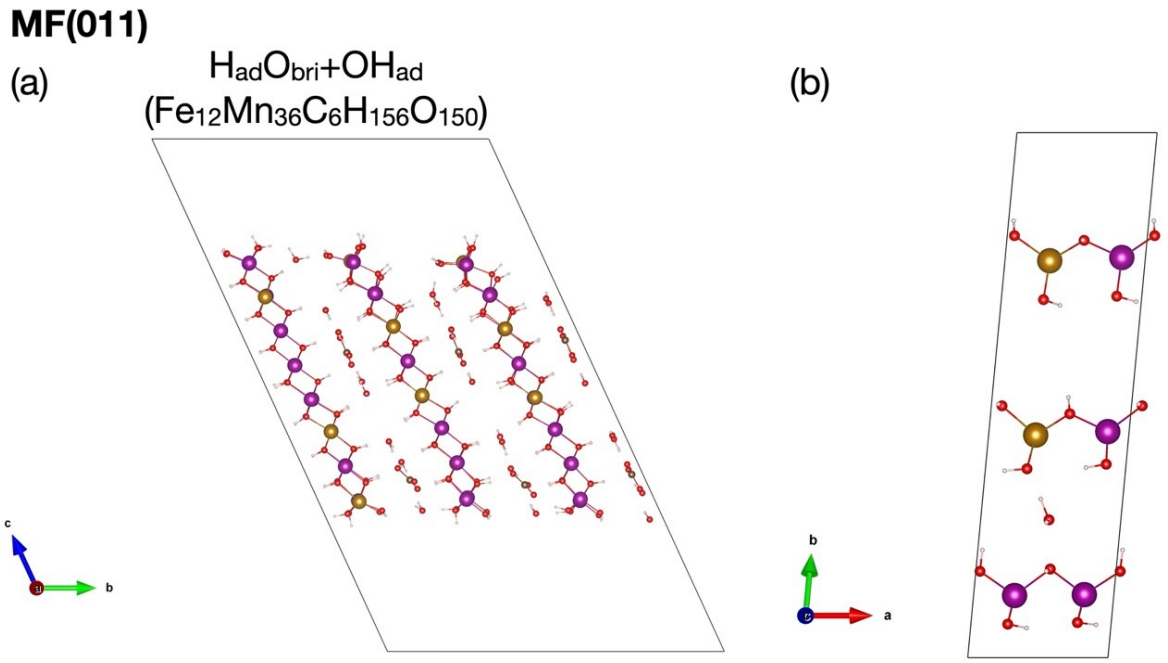

Figure S10. (a) The side view of the $H_{ad}O_{bri}+OH_{ad}$ structure in the MF(011) surface. (b) The surface sites of the corresponding structure from the top view.

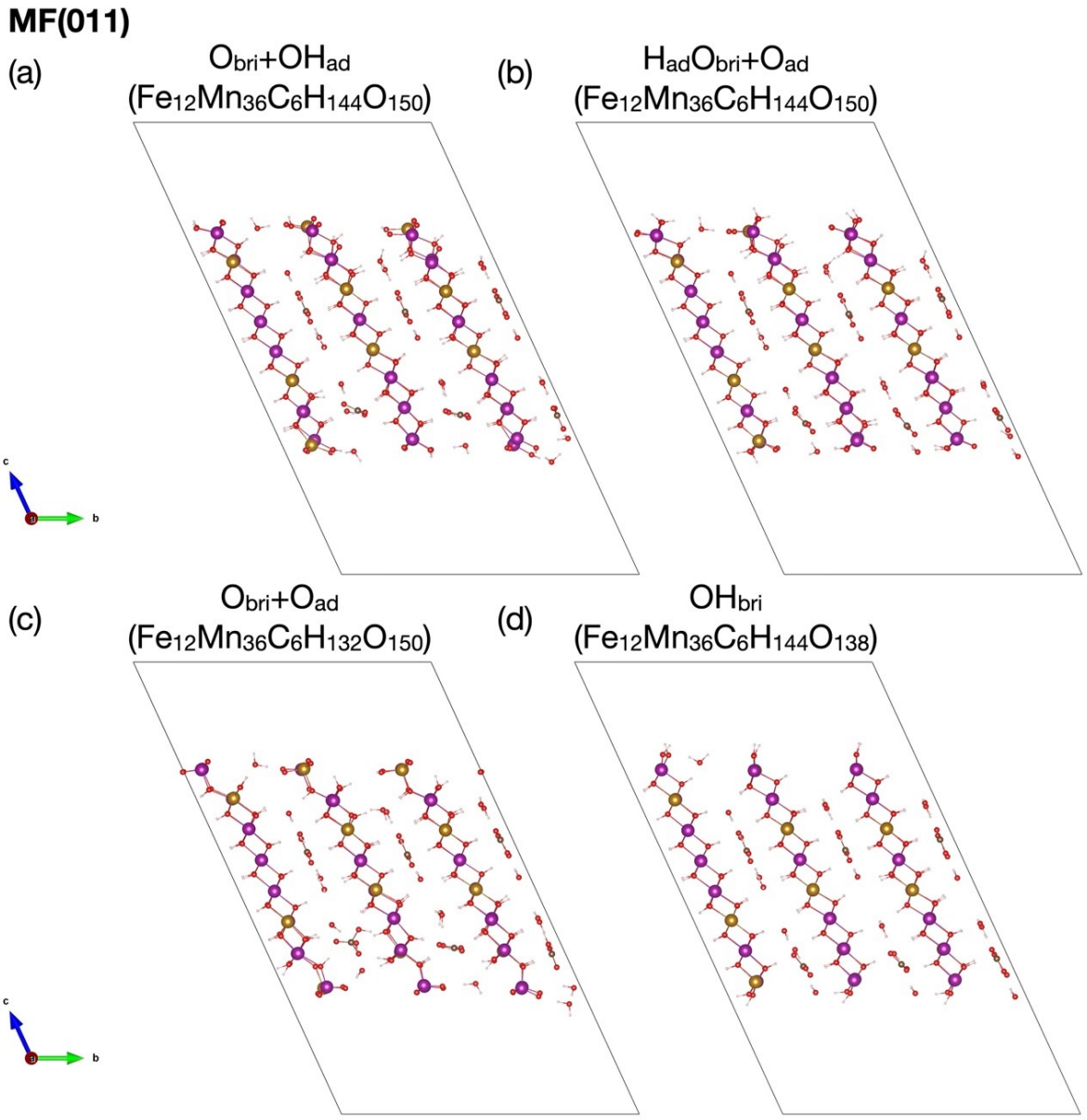

Figure S11. The side views of (a) O_{bri}+OH_{ad}, (b) $H_{ad}O_{bri}$+O_{ad}, (c) O_{bri}+O_{ad}, and (d) OH_{bri} in the MF(011) surface.

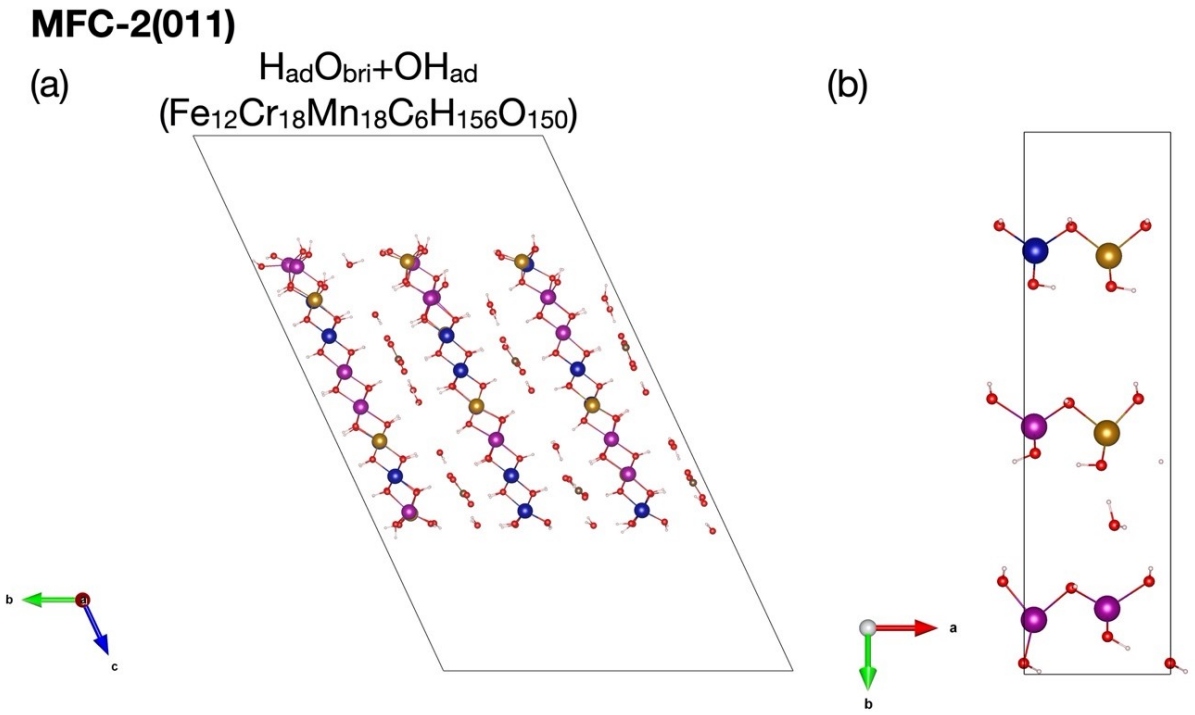

Figure S12. (a) The side view of the $H_{ad}O_{bri}+OH_{ad}$ structure in the MFC-2(011) surface. (b) The surface sites of the corresponding structure from the top view.

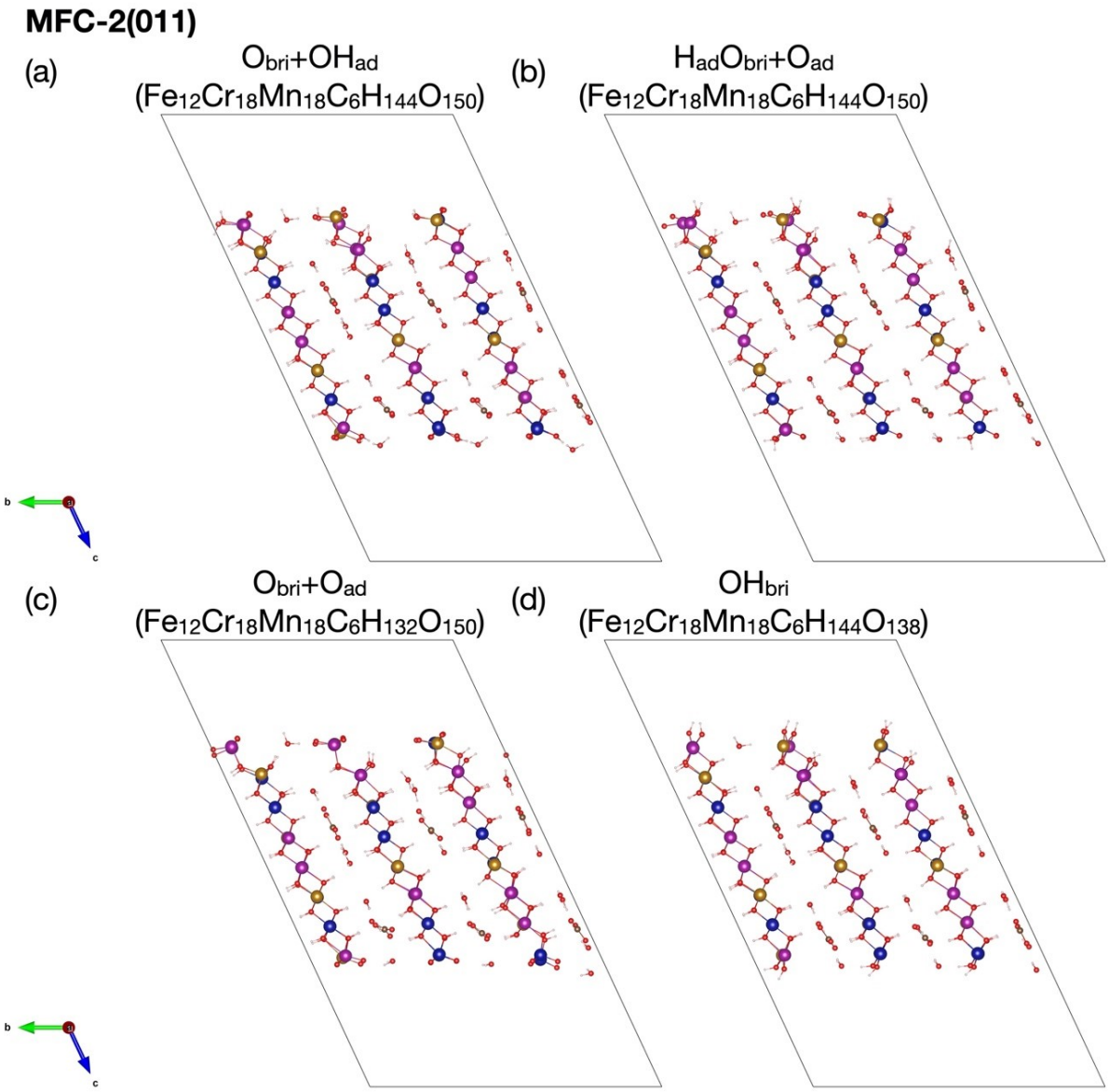

Figure S13. The side views of (a) O_{bri}+OH_{ad}, (b) $H_{ad}O_{bri}$+O_{ad}, (c) O_{bri}+O_{ad}, and (d) OH_{bri} in the MFC-2(011) surface.

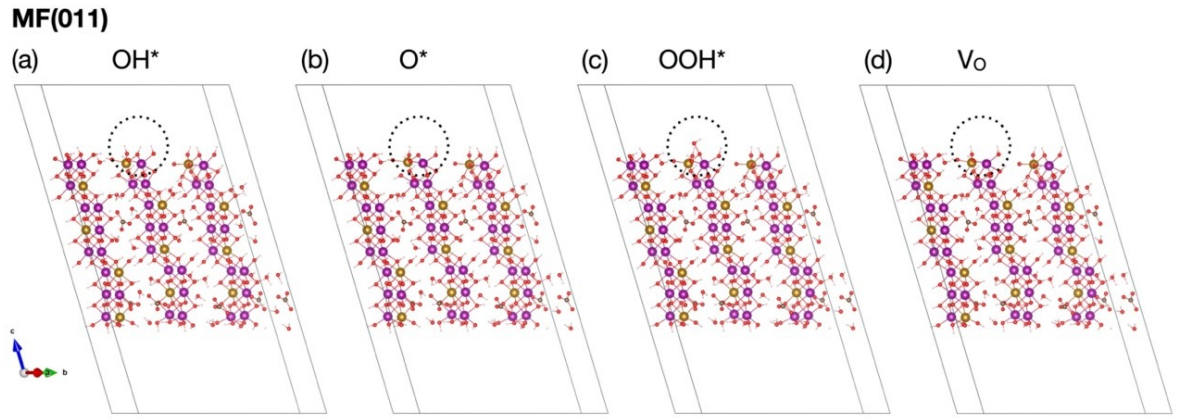

Figure S14. The intermediate structures of OER in the MF(011) surface using the $H_{ad}O_{bri}$+OH_{ad} termination.

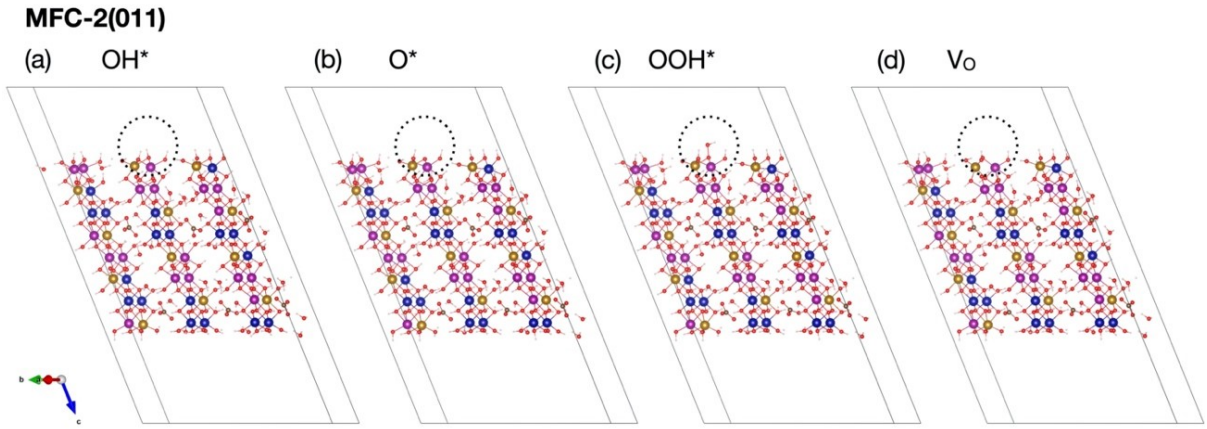

Figure S15. The intermediate structures of OER in the MFC-2(011) surface using the $H_{ad}O_{bri}$+OH_{ad} termination.

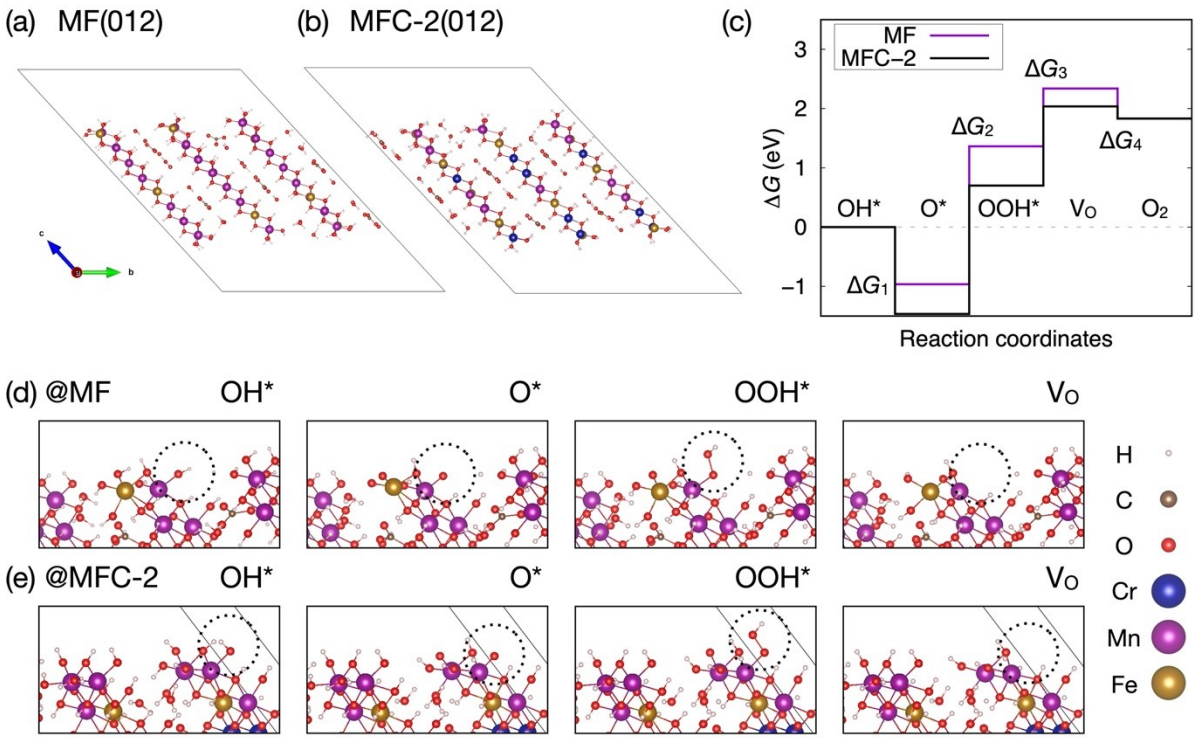

Figure S16. The side views of (a) MF(012) and (b) MFC-2(012) slab models. (c) Calculated Gibbs free energy profiles of OER via the Mars van Krevelen mechanism under alkaline condition. The intermediate adsorbed structures of (d) MF(012) and (e) MFC-2(012).

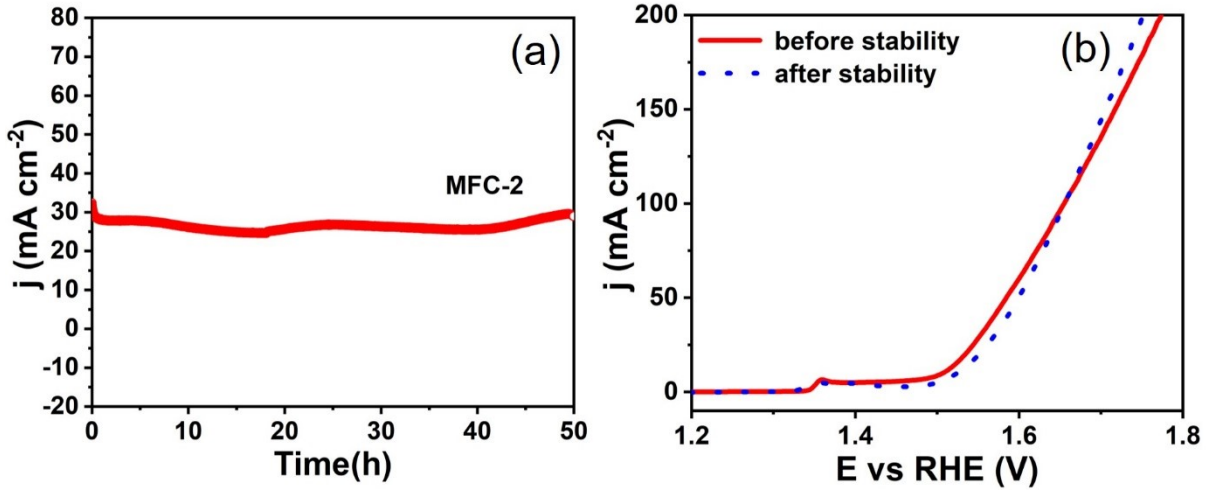

Figure S17. (a) Chronoamperometry study of MFC-2 for OER in alkaline real seawater and (b) corresponding LSV plots before and after stability test.

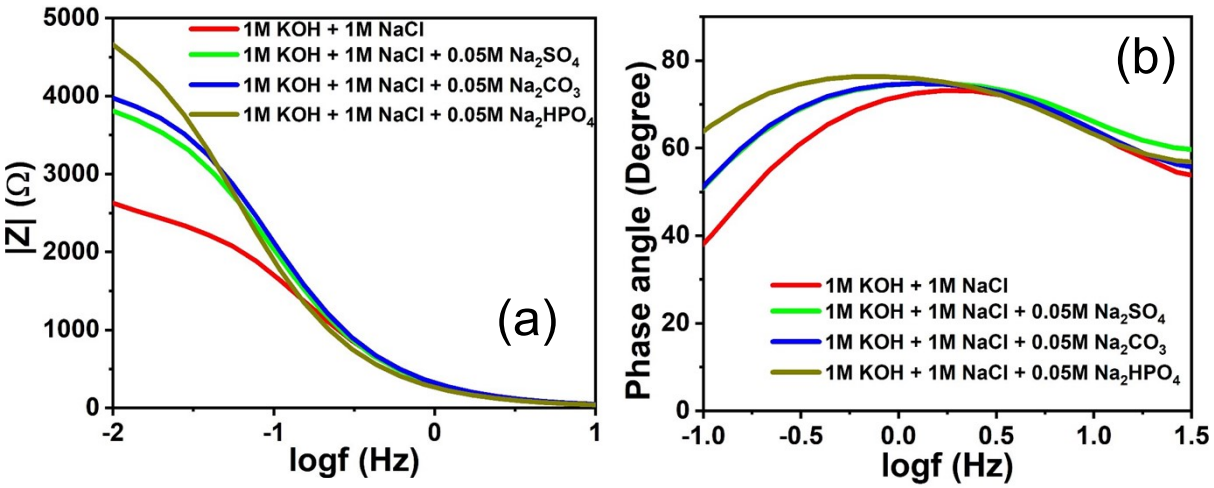

Figure S18. (a) Bode plot and (b) Phase angle plot of MFC-2 LTH in presence and absence of different corrosion inhibitors in 1M KOH + 1M NaCl electrolyte.

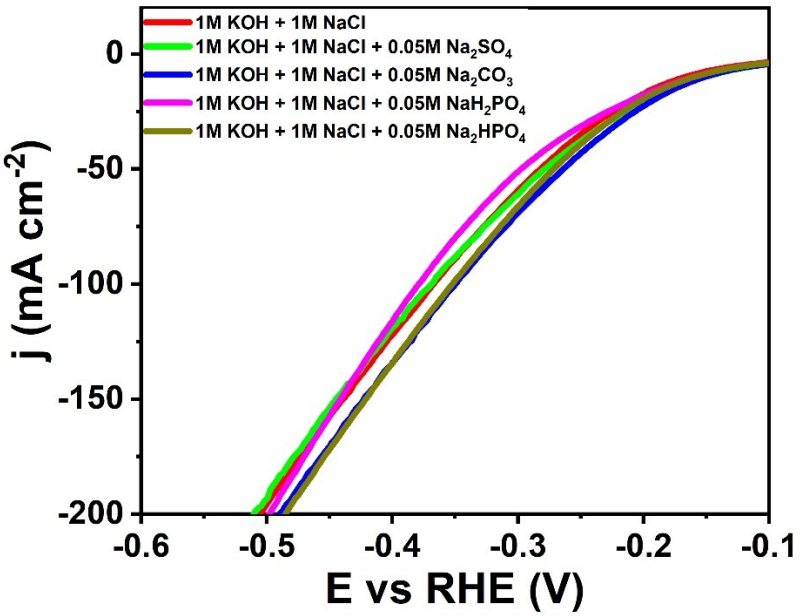

Figure S19. LSV plots of MFC-2 for HER in 1M KOH + 1M NaCl with and without inhibitors showing no noticeable influences.

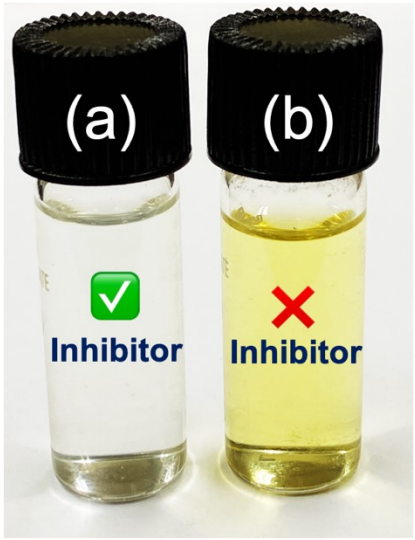

Figure S20. Iodometry test confirming a) no formation of ClO^- due to CER in presence of carbonate inhibitor and b) formation of ClO^- as indicated by yellow coloration in absence of carbonate in real seawater after chronopotentiometry test.

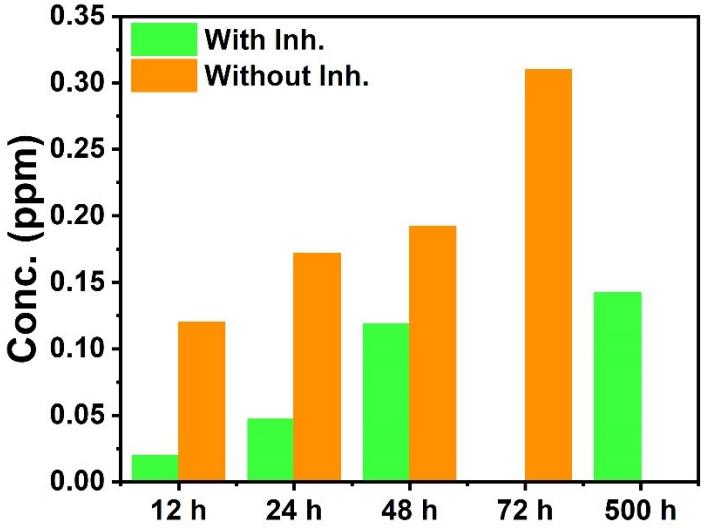

Figure S21. Comparative bar diagram showing concentration of oxidants including hypochlorite determined by DPD test in colorimetric method during seawater electrolysis in presence and absence of inhibitor at certain intervals of long run stability test. The calibration has been made based on standard permanganate solution.

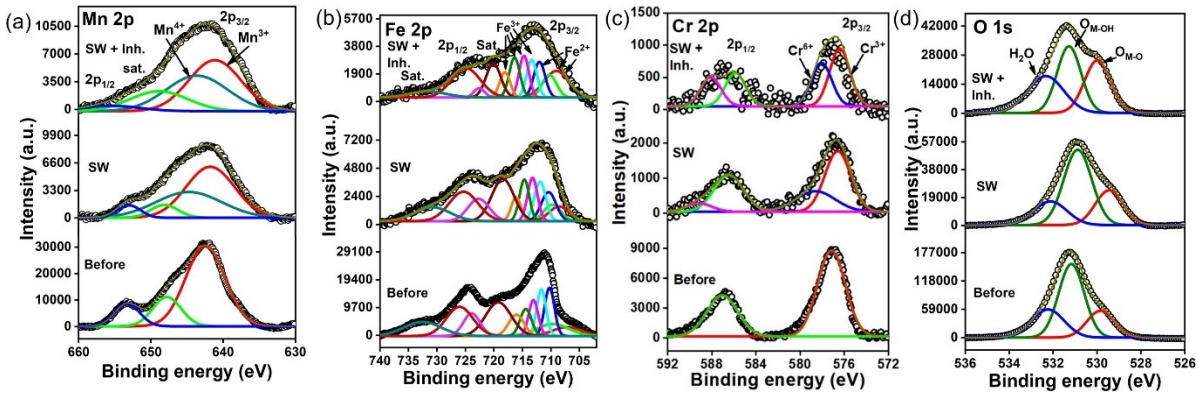

Figure S22. XPS spectra of (a) Mn 2*p*, (b) Fe 2*p*, (c) Cr 2*p* and (d) O 1*s* after prolonged stability for OER in seawater with and without inhibitor.

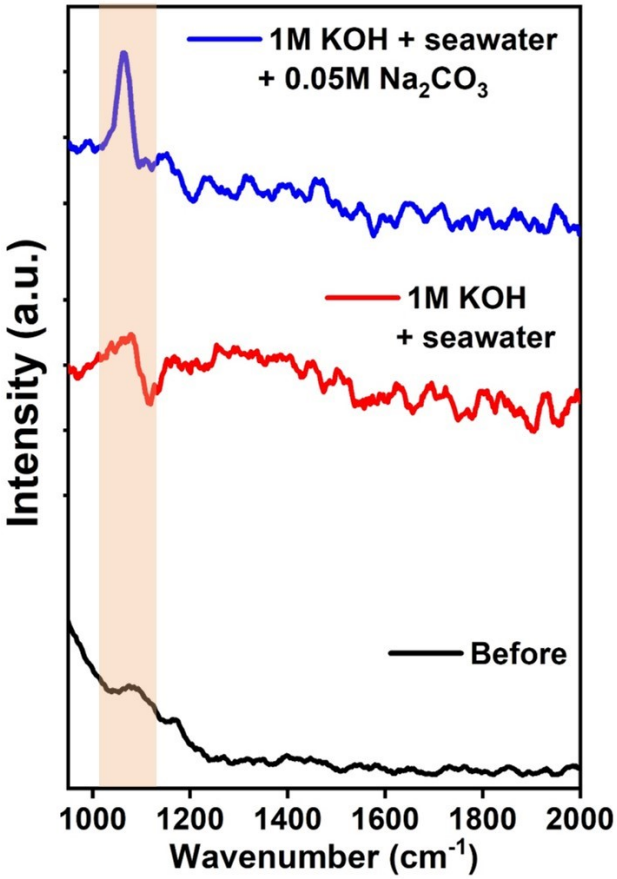

Figure S23. Raman Spectroscopy of MFC-2 LTH before and after prolonged stability for OER in seawater with and without inhibitor. The shaded area indicates presence of CO_3^{2-}.

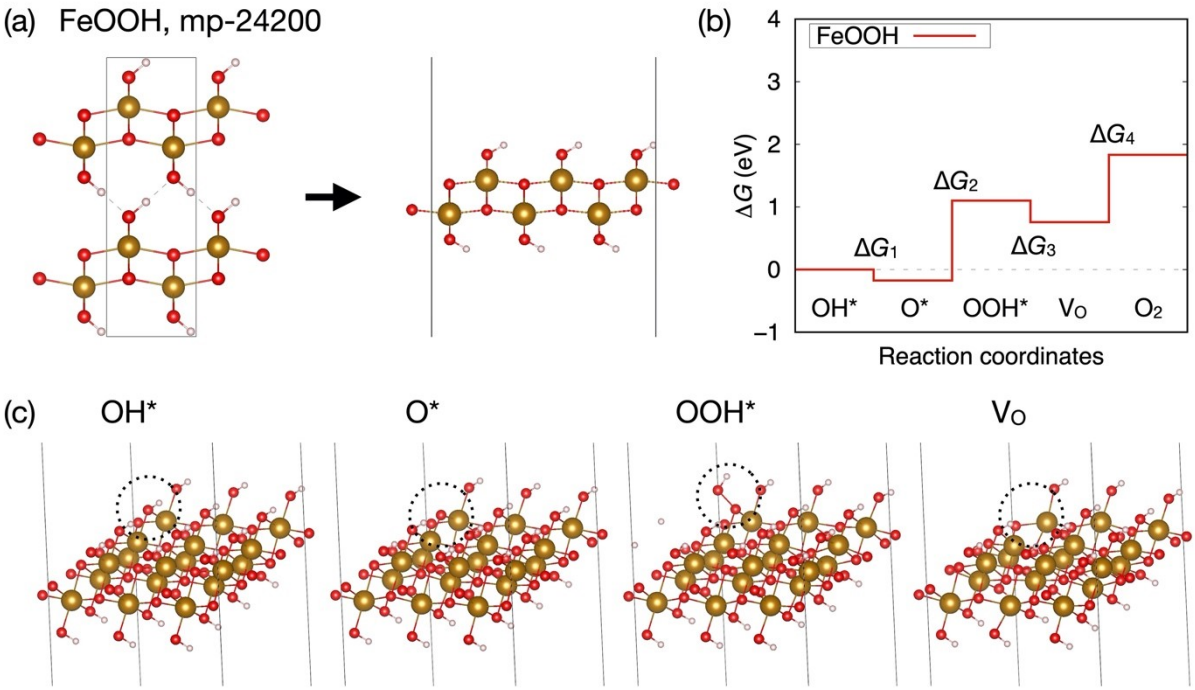

Figure S24. (a) A thin layer model of FeOOH generated from bulk structural information provided by the Materials Project database (mp-24200). (b) Calculated Gibbs free energy profile of OER via the Mars van Krevelen mechanism under alkaline condition and (c) the intermediate adsorbed structures. 2×2×1 sampling meshes were used for the Brillouin-zone integration while the other computational conditions were the same as those described in the main text.

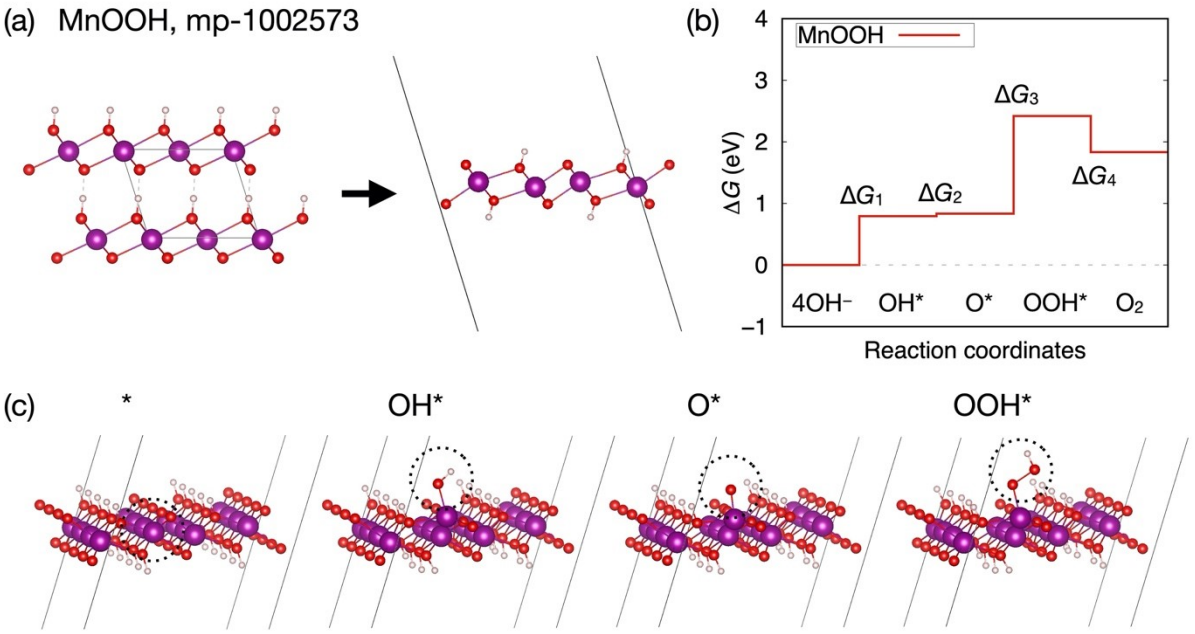

Figure S25. (a) A thin layer model of MnOOH generated from bulk structural information provided by the Materials Project database (mp-1002573). (b) Calculated Gibbs free energy profile of OER under alkaline condition and (c) the intermediate adsorbed structures. 2×2×1 sampling meshes were used for the Brillouin-zone integration while the other computational conditions were the same as those described in the main text.

Table S1. Reaction parameters and precursor concentrations used for developing LDH and LTHs.

Samples	Reaction Temp/Time	Mn (mM)	Fe (mM)	Cr (mM)	Total Precursor Conc. (mM)
MF	120 °C/16h	1	3	--	4
MFC-1		0.75	3	0.25	4
MFC-2		0.5	3	0.5	4
MFC-3		0.25	3	0.75	4

Table S2. Elemental information for developed LDH and LTHs based on the EDX analysis.

Samples	Mn (at%)	Fe (at%)	Cr (at%)	O (at%)
MF	5	14.2	0	80.8
MFC-1	3.9	19.1	1.8	75
MFC-2	2.6	21.1	2.6	73.7
MFC-3	1.6	20.1	5.5	72.8

Table S3. Electrochemical Impedance Spectroscopy (EIS) parameters of fitted data of various electrocatalysts in 1M KOH electrolyte at 287 mV overpotential for OER process.

Sample	R_s (Ohm)	R_{ct} (Ohm)
MF	1.11	2.88
MFC-1	0.83	1.09
MFC-2	0.54	0.55
MFC-3	0.98	1.23
RuO_2	1.5	9.2

Table S4. Fitted simulation EIS result with R_s, R_c, R_{ct}, Y and n parameters of MFC-2 in presence and absence of inhibitors in 1M KOH + 1M NaCl electrolyte.

Electrolyte	R_s (Ωcm^2)	R_c (Ωcm^2)	Y_1 ($\Omega^{-1}cm^{-2}$)	n_1	R_{ct} (Ωcm^2)	Y_2 ($\Omega^{-1}cm^{-2}$)	n_2
1 M KOH + 1 M NaCl	0.65	6.90	1.20×10^{-3}	0.83	1530	1.28×10^{-3}	0.90
1 M KOH + 1M NaCl + 0.05 M Na_2SO_4	0.73	15.99	0.928×10^{-3}	0.805	2312	1.09×10^{-3}	0.93
1 M KOH + 1M NaCl + 0.05 M Na_2CO_3	0.85	14.50	0.846×10^{-3}	0.81	2484	1.05×10^{-3}	0.91
1 M KOH + 1M NaCl + 0.05 M Na_2HPO_4	0.73	19.28	0.934×10^{-3}	0.80	2912	1.02×10^{-3}	0.93

Table S5. Potentiodynamic polarization (PD) parameters of MFC-2 LTH in different electrolyte solutions.

Electrolyte	E_{corr} (V)	β_a (V/dec)	β_c (V/dec)	R_p ($\Omega.cm^2$)	Corrosion rate(mm/year)	η (%)
1M KOH + 1M NaCl	0.843	2.8604	1.1868	809.75	5.2273	---
1M KOH + 1M NaCl + 0.05 M Na_2SO_4	0.861	0.71996	0.26822	2584.8	0.69549	68.7
1M KOH + 1M NaCl + 0.05 M Na_2CO_3	0.857	0.49235	0.24042	2690.75	0.88123	69.9
1M KOH + 1M NaCl + 0.05 M Na_2HPO_4	0.866	2.6003	0.12209	2539.8	0.2317	68.1

Table S6. Fitted data of EIS spectroscopy of various electrocatalysts in 1M KOH electrolyte at 230 mV overpotential for HER process.

Electrocatalyst	R_s (ohm)	R_{ct} (ohm)
MFC-1	1.1	7.5
MFC-2	0.56	3.08
MFC-3	1.02	7.22
MF	1.12	14.75
Pt/C	1.4	11.87

Table S7. Comparison of C_{dl}, ECSA and TOF of developed electrocatalysts in 1M KOH medium.

Catalyst	C_{dl} at -0.15 V (mF cm^{-2})	ECSA	TOF (s^{-1}) at η_{300}
MF	1.41	12.8	0.019
MFC-1	1.57	18.42	0.047
MFC-2	2.25	22.93	0.106
MFC-2	1.48	13.67	0.042

Table S8. pH monitoring over the stability periods in alkaline seawater electrolyte with and without inhibitor.

Duration for stability study (h)	pH of electrolyte	
	Alkaline seawater	Alkaline seawater + Inhibitor
0	13.9	13.9
5	13.8	13.84
24	13.8	13.83
48	13.78	13.80
72	13.75	--
500	--	13.75

Table S9. Comparative electrocatalytic performances of recently developed electrocatalysts for seawater splitting.

Catalysts	Electrolyte	OER		HER		Overall		Ref
		η_{OER} (mV) @ J (mA.cm^{-2})	Durability (h)	η_{HER} (mV) @ J (mA.cm^{-2})	Durability (h)	Cell Voltage (V) @ J (mA.cm^{-2})	Durability (h)	
S-(NiFe)OOH	1M KOH + Seawater	300@100	100	--	--	--	--	S1
NiFe LDH	0.1M KOH + 0.5M NaCl	359@10	120	--	--	--	--	S2
NiFe LDH	0.1M KOH + 0.5M NaCl	270@10	100	--	--	--	--	S3
NiFe hydroxide/Ni S_x-Ni ||Ni-NiO Cr_2O_3	1M KOH + 0.5M NaCl	300@400	1000	160@500	22	2.08@400	500	S4
	1M KOH + seawater	--	--	--	--	2.12@400	1000	
B-CoFe LDH	1M KOH + Seawater	310@100	100	--	--	--	--	S5
N-CDs/NiFe LDH	1M KOH + 0.5M NaCl	285@100	20	--	--	--	--	S6
	1M KOH + seawater	340@100	20	--	--	--	--	
CoPx||CoPx FeOOH	1M KOH + Seawater	283@100	83	190@100	--	1.71@100	80	S7
CoFeZr LDH/NF	1M KOH + 0.5M NaCl	303@100	30	--	--	1.66@15	20	S8
NiMoN@ NiFeN	1M KOH + 0.5M NaCl	286@100	--	--	--	1.56@100	100	S9

	1M KOH + seawater	307@100		82@100	--	1.58@100	100	
HCl-c-NiFe LDH	1M KOH + 0.5M NaCl	178@100	--	175@100	--	1.81@500	300	S10
NiFe-LDH	1M NaOH + Seawater	333@100	--	--	--	--	--	S11
	1M NaOH + 0.5M NaCl + 0.05M Na_2SO_4	--	--	--	--	2.3@400	1000	
MnFeCr LTH	1M KOH + 1M NaCl	303@100 332@300	--	277@100 362@300	--	--	--	**This work**
	1M KOH + seawater	341@100 424@300	50	292@100 347@300	70	2.30@300	72	
	1M KOH + seawater + 0.05M Na_2CO_3	--	--	--	--	2.27@300	500	

Table S10. ICP-MS analysis of electrolytes after stability test of MFC-2 at current density of 300 mA cm^{-2}.

Metals	**Concentration in electrolyte solution (ppm)**	
	In presence of inhibitor	**In absence of inhibitor**
Mn	<0.000	0.001
Fe	<0.000	<0.000
Cr	0.012	0.050

Table S11. Calculated Gibbs free energy changes of OER under alkaline condition. The asterisk marks indicate the reactions via the Mars van Krevelen mechanism.

Surfaces	Intermediates			
	ΔG_1	ΔG_2	ΔG_3	ΔG_4
MF(012)*	−0.964 eV	**2.33 eV**	0.969 eV	−0.506 eV
MFC-2(012)*	−1.46 eV	**2.17 eV**	1.34 eV	−0.205 eV
FeOOH*	−0.175 eV	**1.28 eV**	−0.343 eV	1.08 eV
MnOOH	0.793 eV	0.0402 eV	**1.59 eV**	−0.587eV

References

S1 L. Yu, L. Wu, B. McElhenny, S. Song, D. Luo, F. Zhang, Y. Yu, S. Chen, Z. Ren, *Energy Environ. Sci.*, 2020, **13**, 3439-3446 .

S2 F. Dionigi, T. Reier, Z. Pawolek, M. Gliech, P. Strasser, *ChemSusChem* 2016, **9**, 962–972.

S3 S. Dresp, F. Dionigi, S. Loos, J.F. de Araujo, C. Spori, M. Gliech, H. Dau, P. Strasser, *Adv. Energy Mater.* 2018, **8**, 1800338.

S4 Y. Kuang, M. J. Kenney, Y. Meng, W. Hung, Y. Liu, J. Huang, R. Prasanna, P. Li, Y. Li, L. Wang, M.C. Lin, M. D. McGehee, X. Sun, H. Dai, *Proc. Natl. Acad. Sci.* 2019, **116**, 6624−6629.

S5 L. Wu, L. Yu, Q. Zhu, B. McElhenny, F. Zhang, C. Wu, X. Xing, J. Bao, S. Chen, Z. Ren, *Nano Energy* 2021, **83**, 105838.

S6 P. Ding, H. Song, J. Chang, S. Lu, *Nano Research* 2022, **15**, 7063-7070.

S7 L. Wu, L. Yu, B. McElhenny, X. Xing, D. Luo, F. Zhang, J. Bao, S. Chen, Z. Ren, *Appl. Catal. B Environ.* 2021*,* **294**, 120256*.*

S8 W. Liu, K. Jiang, Y. Hu, Q. Li, Y. Deng, J. Bao, Y. Lei, *J. Colloid Interface Sci.* 2021, **604**, 767.

S9 L. Yu, Q. Zhu, S.W. Song, B. McElhenny, D.Z. Wang, C.Z. Wu, Z.J. Qin, J.M. Bao, Y. Yu, S. Chen, Z. F. Ren, *Nat. Commun.* 2019, **10**, 5106.

S10 S. Duan, Z. Liu, H. Zhuo, T. Wang, J. Liu, L. Wang, J. Liang, J. Han, Y. Huang, Q. Li, *Nanoscale* 2020, **12**, 21743-21749.

S11 T. Ma, W. Xu, B. Li, X. Chen, J. Zhao, S. Wan, K. Jiang, S. Zhang, Z. Wang, Z. Tian, Z. Lu, L. Chen, *Angew. Chem. Int. Ed*., 2021, **60**, 22922-22926.